

Design and Development of Novel Anticancer Peptide Encapsulated Liposomes for Targeting of Solid Tumours *In Vitro*

Lusanda Mtetwa ¹, Nkeiruka Igbokwe ¹, Eman Ismail Abdallah ¹, Makabongwe Mazibuko ², Aviwe Ntsethe ³, Londiwe Simphiwe Mbatha ¹, Terisha Ghazi ², Anil Chuturgoon ², and Mbuso Faya ^{1*}

¹Discipline of Pharmaceutical Sciences, College of Health Sciences, University of KwaZulu-Natal, Private Bag X54001, Durban, South Africa

²Discipline of Medical Biochemistry, College of Health Sciences, University of KwaZulu-Natal, Private Bag X54001, Durban, South Africa

³School of Laboratory Medicine and Medical Sciences, College of Health Sciences, University of KwaZulu-Natal, Private Bag X54001, Durban, South Africa

***Corresponding Author:** Mbuso Faya, Discipline of Pharmaceutical Sciences, College of Health Sciences, University of KwaZulu-Natal, Private Bag X54001, Durban, South Africa

Received Date: April 25, 2025 | **Accepted Date:** May 07, 2025 | **Published Date:** May 15, 2025

Citation: Lusanda Mtetwa, Nkeiruka Igbokwe, Eman I. Abdallah, Makabongwe Mazibuko, Aviwe Ntsethe, et al, (2025), Design and Development of Novel Anticancer Peptide Encapsulated Liposomes for Targeting of Solid Tumours *In Vitro*, *International Journal of Clinical Case Reports and Reviews*, 25(5); DOI:10.31579/2690-4861/589

Copyright: © 2025, Mbuso Faya. This is an open-access article distributed under the terms of the Creative Commons Attribution License, which permits unrestricted use, distribution, and reproduction in any medium, provided the original author and source are credited.

Abstract:

Conventional cancer treatments possess limitations for solid tumours, such as lack of selectivity, thus nanomedicine is explored as an efficient tool in anticancer drug development. Therefore, this study aimed to design a novel anticancer peptide (ACP) and encapsulate it into a lipid-based nanoparticle for efficient delivery to tumours. ACP was designed using *in silico* methods and thereafter encapsulated into a liposomal formulation (P1CF1) using a thin-film hydration method. The shape, size, polydispersity index (PDI), and zeta potential (ZP) of the formulation were evaluated using cryo-transmission electron microscopy, and zetasizer, while the percentage drug encapsulation efficiency (%EE) and drug release were investigated using the ultra-filtration and the dialysis methods. The biocompatibility, cytotoxicity, and apoptosis activity of P1CF1 were evaluated using hemolysis, 3-[(4,5-dimethylthiazol-2-yl)-2,5-diphenyl tetrazolium bromide] and annexin V-FITC/PI assays. P1CF1 was spherical, had a size of 193.46 ± 0.10 nm, a PDI of 0.342 ± 0.12 , a ZP of -7.67 ± 0.04 mV, and an %EE of $91.23 \pm 0.01\%$. Furthermore, P1CF1 was biocompatible at low concentrations, showed a controlled *in vitro* drug release, induced high cytotoxic (IC₅₀ value of 2.967 µg/ml) and apoptosis effects on the cancer cells MCF-7 and was well tolerated by non-cancer HEK293 cells (IC₅₀ value of 135.3 µg/ml). Overall, P1CF1 showed efficient encapsulation capacity, enhanced biocompatibility, and significant anticancer activity in tumour cells with minimum effect on healthy cells. These positive characteristics indicate potential *in vivo* applicability. Thus, future research can include *in vivo* evaluation of this novel formulation.

Key words: anticancer peptides; liposomes; formulation; solid tumours

Introduction

Cancer is a significant public health challenge as it is the second-leading cause of death in the world [1]. From the many available cancer treatment modalities, chemotherapy is regarded with greater significance in cancer treatment options and will most likely remain so for many decades to come [2]. However, though cancer therapy with conventional chemotherapeutic drugs has some benefits, the direct administration of chem-drugs is associated with severe limitations, such as rapid elimination, low bioavailability, lack of specificity, which can result in systemic toxicity and adverse consequences; and multidrug resistance

(MDR), which can lead to recurring, unresponsive tumors and inadequate drug dose, which can impede certain apoptotic pathways and hinder cell death processes [3-6]. Thus, methods to address these challenges are still required.

The use of lipid-based delivery systems such as liposomes as drug carriers in nanomedicine has gained popularity due to their sophistication and attractive traits [7]. These include flexibility, ease of synthesis, reliability, versatility, nano-size (50-500 nm), biocompatibility, enhanced bioavailability, biodegradability, the capacity to shield payloads from

intracellular enzyme degradation; targeted drug delivery to tumor tissues; enhanced effectiveness and therapeutic index; the capacity to encapsulate drugs that are both hydrophilic and hydrophobic; high levels of drug loading and entrapment efficiency; regulated drug release profiles; reduced toxicity of the encapsulated drugs; enhanced pharmacokinetic effects including reduced excretion, prolonged circulation lifespans; and ability to be tailor-designed for targeted drug delivery [8-12]. Because of the leaky nature of tumor tissue capillaries, these vesicles' spherical form and micro size allow them to extravasate and passively accumulate in cancer regions, a phenomenon known as the increased permeability and retention (EPR) effect [13]. To date, numerous liposome formulations have been approved for cancer therapy, including Onivyde™, Marqibo®, Doxil®, Visudyne®, and Depocyt® [14]. Future research and innovation in liposomal drug delivery systems hold considerable potential for the advancement of pharmaceuticals and nanomedicine.

The concept of peptide-targeted liposomes is a significant advancement in the usage of liposomal formulations in cancer treatment. Peptides have been identified as attractive and viable targeting ligands for directing liposomes to target tumours and sequentially enhancing the selectivity and specificity of drug-loaded liposomes, minimizing off-target delivery [15, 16]. This is supported by many *in vivo* and *in vitro* research that have been documented over the years [16-24]. However, there is a huge gap in the literature and drug development focussing on liposomal encapsulation of anticancer peptides (APCs) that target solid tumours.

Recently, ACPs have vastly become a developing approach in nanomedicine, particularly, in drug development. These are a series of short amino acids, with anticancer properties which are alternatives to chemo-drugs used in cancer treatments. These ACPs cause cell death by different mechanisms, such as mediated immunity, membrane disruption apoptosis, DNA synthesis inhibition, hormonal/membrane receptors, and anti-angiogenic [25, 26]. Though these drugs exhibit great anticancer properties, limited studies have been done on them as therapeutic payloads, and this could be due to their lack of bioavailability because of intracellularly degraded following administration. Therefore, extensive research is required to establish whether liposomes can encapsulate these ACPs and deliver them safely and efficiently to tumour sites. Thus, this study aimed to design and advance a novel anti-cancer peptide using computational-aided drug design tools, encapsulate it into a liposome and evaluate its physicochemical features as well as its biological activity *in vitro*.

2. Method and Materials

2.1 Materials

Novel anticancer peptides (sequence: FKKLLAKLAK) were designed in-house using the lead anticancer peptide purchased from ChinaPeptides (QYAOBIO) Ltd, China, by a solid phase peptide synthesis protocol. Cholesterol and phosphatidylcholine that were purchased from Sigma-Aldrich (USA) were used for liposomal preparations. Trifluoroacetic acid (TFA) acetonitrile, phosphate-buffered saline (PBS), dichloromethane, and a dialysis bag with a molecular weight cut-off (MWCO) size of 10,000 Dalton (Da) was purchased from Sigma-Aldrich (USA). All other solvents used were of High-Performance Liquid Chromatography (HPLC) analytical grade and were used without additional purification. Distilled water was used throughout this study and was purified in the laboratory with a Milli-Q purification system (Millipore Corp., USA).

2.2 Methods

Auctores Publishing LLC – Volume 20(5)-589 www.auctoresonline.org
ISSN: 2690-4861

2.2.1 Anticancer Peptide Design

The amino acid sequences of the purified peptides were determined using the automated online software CancerPPD (Database of Anticancer Peptides and Proteins) (<http://crdd.osdd.net/raghava/cancerppd/>) [27]. The peptide sequence FAKLLAKLAK with ID 1854 and a 10 amino acid chain, was used as the anticancer reference sequence that targeted solid tumours - breast cancer. The reference amino acid sequence was incorporated into CellPPD: Designing of Cell Penetrating Peptides (<http://crdd.osdd.net/raghava/cellppd/>) online software to select mutants of the reference compound. A mutant peptide was generated with a 10 amino acid length, FKKLLAKLAK. The lead anticancer peptide was then purchased from ChinaPeptides (QYAOBIO) Ltd., China The sequence FKKLLAKLAK (Phe-Lys-Lys-Leu-Leu-Ala-Lys-Leu-Ala-Lys) was identified with a purity of 98.28% and was soluble at 1 mg/ml in 17% acetonitrile (ACN)/83% water (H₂O).

2.2.2 Liposome Preparation

Liposomes were prepared using a thin-film hydration technique [28]. The liposome thin film layer was prepared at a 6:4 ratio of PC (phosphatidylcholine) and cholesterol, respectively. Briefly, 6 mg of PC and 4 mg of cholesterol were dissolved in 3 ml of dichloromethane (DCM) and added into a round-bottom flask. To ensure homogenous mixing, the dissolved lipid combination was vortexed for 1 min, and 20 small (1-2cm) glass beads were added. The mechanism of using glass beads was to ensure thorough mixing and to obtain a thin uniform film. The solvents were then evaporated using a rotatory evaporator for 25 mins at 40°C to obtain a thoroughly dried thin film layer. The thin film was further dried in a vacuum-pressure desiccator for 48 hrs. The dried thin lipid film was then hydrated with 5 mg of the anticancer peptide that was dissolved in 5 ml of distilled water. The hydrated lipid film was vortexed for 1min and let to stand for a long hydration of 2hrs, this was done to achieve adequate encapsulation of the peptide within the lipid film. Thereafter the hydrated liposome formulation was filtered using a 0.45 µm nylon syringe filter. Next, the rehydrated thin film was sonicated in ice for 10 mins at 30% amplitude using a probe sonicator (Omni Sonic-Ruptor 400 Ultrasonic Homogenizer, USA).

2.2.3 Physicochemical Characterization of ACP Encapsulated Liposomes

2.2.3.1 Morphology, Particle Size, Polydispersity Index and Zeta Potential

The liposome shape was observed using cryo-TEM (Joel, JEM-1010, Tokyo, Japan). The liposome formula was frozen at -183°C to maximize the formation of vitreous ice. After that, the grid containing the vitrified film was placed under the microscope and studied in transmission mode at the temperature of liquid nitrogen. Their ZP, PDI, and particle size were examined via dynamic light scattering using a Zetasizer Nano ZS90 (Malvern Instruments Ltd, UK) at 25°C in polystyrene cuvettes. Dilutions were made of 900 µl of distilled water, and 100µl of prepared liposome formulation. Every measurement was done three times.

2.2.4 Determination of Encapsulation Efficiency Percentage

The ultrafiltration method was evaluated to determine the concentration of anticancer peptide encapsulated within the liposome. This ultrafiltration method used Amicon® Ultra-4, centrifugal filter tubes (Millipore Corp., USA) with 10 kDa pore size and centrifuged at 3000 rpm at 25°C for 15 mins to receive the untrapped concentration. Then,

500 μ l of liposome was diluted in 1 ml of ACN and bath sonicated to properly break down the system to detect the value of the entrapped drug. The encapsulation efficiency of the liposome was determined using reverse-phase high-performance liquid chromatography (RP-HPLC) LC-2050C 3D PDA detector, autosampler with LC/GC solution 5.106 SPI system software Shimadzu (Kyoto, Japan). The mobile phase A 0.1% trifluoroacetic acid (TFA) in water and mobile phase B graded 100% ACN was used with a Kromasil 100-5C18, 4.6mmx250mm, 5-micron column at 25°C. The flow rate was set at 0.5 ml/min with the wavelength set at 280 nm and an injection volume at 10 μ l. The regression equation of $y=5045,2x$ and the linearity coefficient (R^2) of 0.9982 was found. The entrapment efficiency was then calculated using the equation (1) below:

$$\text{Entrapment Efficiency (\%)} = \frac{\text{Actual amount of drug in nanoparticle} - \text{Unentrapped amount}}{\text{Actual amount of drug in nanoparticle}} \times 100 \quad (1)$$

2.2.5 In Vitro Hemolysis Testing

The hemolysis effect of different concentrations of ACP-encapsulated liposomes was indirectly assessed by both a visual examination and by detecting the optical absorbance provided by the released hemoglobin present in the supernatant, as previously described [29], with minor modifications. Briefly, the NHLS antivenom sheep blood was washed three times with 0.01M PBS solution (pH 7.4) followed by centrifugation (4DE centrifuge, Centurion Scientific Ltd, UK) at 3000 rpm for 10 mins. For each of the samples, liposome formulation was diluted with PBS for concentrations that ranged from 0.05 to 0.5 mg/ml. The red blood cell (RBC) suspension of 200 μ l was then added to 1800 μ l of each sample and left to incubate for 30 mins at a normal body temperature of 37°C. Thereafter, the samples went through further centrifugation at 3000 rpm for 10 mins. After centrifugation, from each sample, the supernatant was collected for readings using a SpectraMax M2 (Molecular Devices, Sunnyvale, CA, USA) at 576 nm to determine the amount of hemoglobin released in the supernatant [30]. To obtain 0% and 100% hemolysis, 200 μ l of RBC suspension was added to 1800 μ l of PBS and distilled water, respectively, as controls. The degree of hemolysis was calculated using equation (2) below:

$$\text{Hemolysis (\%)} = \frac{(\text{Abs}_{100} - \text{Abs}_0)}{\text{Abs}_{100} - \text{Abs}_0} \times 100 \quad (2)$$

where Abs_{100} and Abs_0 are the absorbances of the samples at 100% and 0% hemolysis, respectively.

2.2.6 In Vitro Drug Release Analysis

The dialysis bag technique was used for the assessment of the anticancer peptide encapsulated liposomal formulation and the bare peptide. Initially, 2 ml (X3) of the bare peptide and 2 ml (X3) of the liposome formulation were carefully loaded into 6 different dialysis bags that had a pore size of 10,000 Da. The loaded dialysis bags were placed in receiver glass containers containing 20 ml PBS (pH 7.4 and 6.0) and were carefully placed in a shaking incubator at 100 rpm with a temperature of 37°C. Then, 2 ml released samples were drawn out from the receiver solution at different time intervals of 0, 2, 4, 6, 8, 12, 24, and 72 hrs and immediately replaced with PBS that is equivalent to the extracted volume, ensuring the total volume in the container remains at 20 ml. The amount of released bare peptide and liposome was determined by RP-HPLC analysis, and a comparison between the bare peptide and the encapsulated liposome was made to determine if there was a better release. The experiment was

performed in triplicate. The DDSolver software program was used to analyse the drug release data [31].

2.2.8 In Vitro Cytotoxicity Studies

2.2.8.1 Cell Culture Maintenance and Treatment

The human breast cancer cells (MCF-7) (obtained from ATCC, catalogue number HTB) and human embryonic kidney cells (HEK293) normal cells were employed for the cytotoxicity studies. Both MCF-7 and HEK293 cells were cultured in separate 25 cm³ cell culture flasks using Dulbecco's minimum essentials medium (DMEM) supplemented with 10% foetal bovine serum (FBS), 1% L-glutamine, 1% penicillin-streptomycin-fungizone and 25mM of HEPES buffer. Cells were grown under standard tissue culture conditions i.e., 37°C, 95% humidified air, and 5% CO₂ until cells reached acceptable cell confluency ~80% [33].

Stock solutions (10 ml) of ACP encapsulated liposome (P₁CF₁) formulation, with bare peptide and azacitidine were prepared using distilled water. A series of serial dilutions were made for the varying MTT assay concentrations (0 – 200 μ g/ml). A negative control (wells with DMEM and cells only) and a positive control (wells with treatment and cells only) were used in this assay. All assays were performed in triplicate.

2.2.8.2 Methyl Thiazol Tetrazolium Assay (MTT) Analysis

A 3-(4,5-dimethylthiazol-2-yl)-2,5-diphenyltetrazolium bromide tetrazolium colorimetric assay was used to assess the cytotoxicity/cell viability of ACP encapsulated liposome and bare peptide in MCF-7 and HEK293 cells after treatment [34]. Briefly, approximately 20,000 confluent cells (approximately 80% confluency) were incubated overnight after being seeded into 96-well microtitre plates. The cells were then treated with test samples at varying concentrations from 0 – 200 μ g/ml and then incubated at 37°C for 24 hrs. Then, old media was removed, followed by the washing of each well with 0.1M PBS. Thereafter, 20 μ l of MTT salt solution (5mg in 1ml PBS) was then added to each well, together with 100 μ l of DMEM media, and left to incubate for 4 hrs at 37°C. After incubation, media/MTT salt solution was removed, then treated with 100 μ l DMSO, to solubilize the formazan crystals, and then incubated for 1 hr. Lastly, the absorbance or optical density of the test samples was measured at 570 nm using a SpectraMax M2 microplate reader (Molecular Devices, Sunnyvale, CA, USA). Background subtraction was performed using cell-free wells containing just media, with untreated cells serving as a positive control.

The percentage (%) of cell viability was calculated using equation (3) below:

$$\text{Cell viability (\%)} = \frac{\text{Absorbance of treated cells}}{\text{Absorbance of untreated cells}} \times 100 \quad (3)$$

2.2.8.3 Apoptosis Analysis

Apoptosis was identified using flow cytometry and annexin V-fluorescein isothiocyanate (FITC)/propidium iodide (PI) apoptosis detection kit II, in accordance with the manufacturer's instructions (ThermoFisher Scientific, Inc., Randburg, SA). Confluent MCF-7 cells were carefully seeded in 96-well plates and were incubated with test treatments P₁CF₁, bare peptide, and azacitidine for 36 hrs at 37°C in 5% CO₂. After 36 hrs of incubation, cells were washed with PBS, collected by trypsinization, centrifuged, and resuspended in binding buffer from the kit. Thereafter, cells were stained with annexin V-FITC for 10 mins and incubated at room temperature and 5 μ l of PI was added before analysis.

Cells were analyzed by the DxFLEX flow cytometer (Beckman Coulter, Inc., Brea, CA, USA), as reported earlier [35].

2.2.9 Statistical Analysis

All experiments were done in triplicate, and the results were reported as mean \pm standard deviation (SD). One-way ANOVA followed by Tukey's multiple comparison test was used to compare more than three data. Student's *t*-test was used to compare two means. Statistically significant values are represented as $p < 0.05$; non-statistical significance values are represented as *ns*.

3. Results and Discussion

Over the years, therapeutic peptides have seemingly received significant attention from scientists as potential drug candidates [36]. Peptides as therapeutic agents have proved to be favourable for many diseases, including cancer, and their applications have been highly advantageous due to their size, high biocompatibility, simplicity in production, and/or modification together with their capacity to penetrate tumours [37]. Much research has been conducted on novel therapeutic ACPs using *in silico* tools to target various diseases. Consequently, there have been many ACPs that have entered clinical trials but still only a few have been approved.

3.1 Identification and Design of Novel Anti-Cancer Peptides (ACPs)

The ACP was designed using the module CancerPPD database (Database of Anticancer Peptides and Proteins) which has already been validated with anticancer activity [38]. For each peptide on the CancerPPD database, adequate details on the specific assays utilized and the experimentally measured activity of the peptides against different cancer

cell lines are provided [39]. During selection, the peptide sequences needed to be short, thus lengths ranged from 5 - 10 amino acids due to the consideration of synthesis and cost of the peptide. The initially selected sequence was FLAK50 T1 (FAKLLAKLAK), and the strategy for novelty was to adjust the amino acids in the given sequence. The sequence FLAK50 T1 originates from FLAK peptides that are highly rich in Phe, Leu, Ala, and Lys and were compiled in the Owen patent dataset [40]. The peptide targets breast cancer and has chirality L, the sequence was linear and the reported activity was LD₅₀ = 615 μ g/ml. The retrieved sequence from CancerPPD was then taken to CellPPD to develop mutant peptides of the sequence. CellPPD database, which is a support vector machine (SMV), assists by developing and designing cell-penetrating peptides (CPPs), which was essential when looking for mutants of the retrieved sequence [27, 41]. CellPPD allows for the design of single mutant analogues of given peptide sequences and identifies whether they are penetrating cells or not. Additionally, CellPPD also provides the physicochemical properties of the generated mutant peptide. From the retrieved sequence, Ala amino acid was substituted with Lys to generate the mutant peptide. The newly generated peptide had the sequence FKKLLAKLAK (Phe-Lys-Lys-Leu-Leu-Ala-Lys-Leu-Ala-Lys) (Fig 1). The peptide had a molecular weight of 1159.67 and a +4 net charge, which advantageously leads to the destruction of cancer cells by engaging with their anionic cell membrane components [42]. The SVM score was 0.30 and the peptide had a clear CPP prediction. For ACPs, hydrophobicity plays an important role in the peptide's ability to cross membrane barriers and hence exert their anticancer effects [43]. The ACP had a hydrophobicity of -0.17, which was ideal as the peptide showed to be mostly hydrophilic. The hydrophilicity was 0.31 and the hydrophobicity was 0.22.

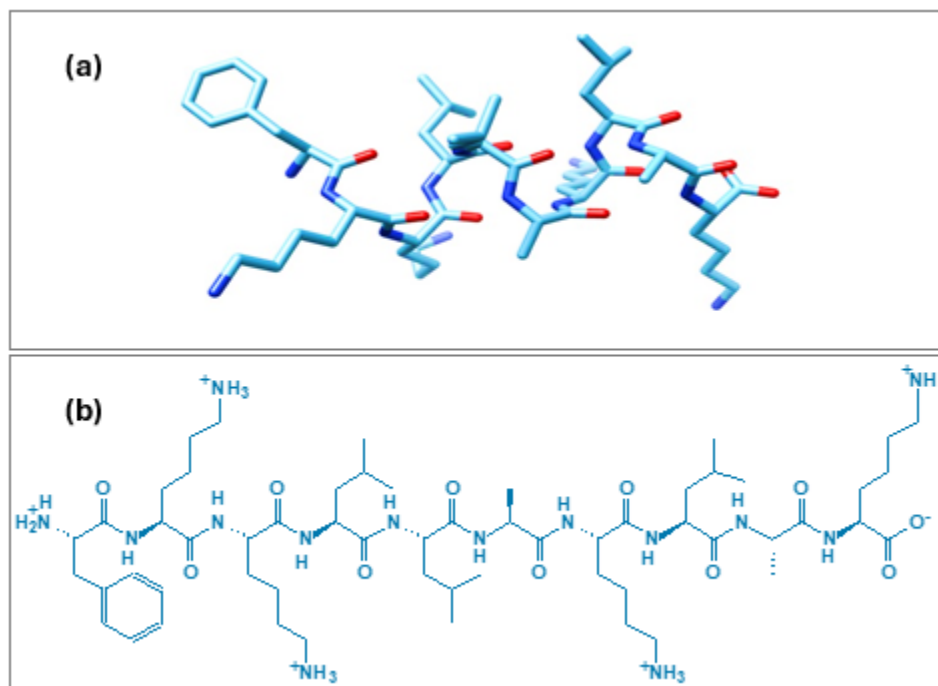


Figure 1: 3D structure (a) and 2D structure (b) of the designed ACP - FKKLLAKLAK (Phe-Lys-Lys-Leu-Leu-Ala-Lys-Leu-Ala-Lys). Images drawn using ChemDraw Software

3.2 Characterisation of ACP Encapsulated Liposomes

3.2.1 Cryo-TEM, DLS-Zeta Sizer

The physicochemical properties of the drug delivery systems have a substantial impact on their tumour permeability, biodistribution, and blood circulation half-life [44]. The ACP-loaded liposome formulations

and blank liposomes (without ACP) were successfully formulated using the thin-film hydration method. A small volume of cholesterol was included in the formulation to increase the stability of the lipid bilayer in biological fluids such as blood plasma [45].

Cryo-TEM images revealed that all formulated liposomes formed spherical structures with similar homogenous sizes (Fig 2). The DLS-Zeta Sizer revealed that the sizes of the liposome formulations ranged from 164 nm – 194 nm, with the blank liposome having a mean diameter size of 164.1 ± 0.11 nm, while the ACP liposome has a slightly larger mean diameter size of 193.4 ± 0.10 nm (Table 1). The increase in size could have been due to the presence of the ACP within the liposome. Studies have shown that NPs larger than 200 nm in diameter tend to activate the complement system, which causes them to leave the bloodstream fast and accumulate in the liver and spleen [44]. Therefore, the formulated liposome sizes fell within the standard size range which is between 100 nm and 200 nm needed for drug delivery through non-specific or receptor-specific endocytosis cellular uptake [46-49]. The use of probe sonication could have had a major influence in obtaining the ideal particle size, as this technique can rearrange and reassemble the lipid content of the liposome to create favourable particle sizes [50]. The PDI value which is correlated to the distribution stability of the formulation, is an important indicator of the overall liposome size distribution [51]. According to literature, PDI values, close to 1.0 are considered not ideal as they may indicate the inverse distribution of the particles and/or the presence of

large particles [52]. Ideally, PDI values should range between 0.30 and low, which indicates that over 60% of the nano-formulations are within the same particle size range and are evenly distributed [51-53]. From the results obtained, the PDI of the blank was below the optimum 0.30, however, the ACP encapsulated liposomes ranged close to the optimum (0.294 ± 0.12 nm to 0.394 ± 0.12 nm) thus showing high-to-medium homogeneity of the liposome mean sizes.

To investigate the physical stability of liposomes, zeta potential was measured. Zeta potential distinguishes the particle surface charge, provides data on the repulsive forces that exist between the particles, and aids in colloidal dispersion stability estimations [54]. Good colloidal stability of nanoparticles is related to ZP values greater than ± 25 mV [55, 56]. All the liposome formulations in the study presented negative ZP values (negative charge), which could be due to the phosphatidylcholine's (used in the thin film) headgroup orientation located at the vesicles surface, and the position of the phosphate group above the choline group plane [57, 58]. The blank liposomes exhibited a ZP of -7.73 ± 0.47 mV, while the ACP liposomes showed a ZP of -7.67 ± 0.04 mV. These findings suggested that the ACP liposome formulation displayed low colloidal stability, which has no profound impact in *in vitro* studies. However, before the application of the formulation *in vivo*, the inclusion of a cationic phospholipid or cationic polymer, helper lipid, and stealth polymer (e.g., polyethylene glycol, PEG) is mandatory for improved colloidal stability and longer circulation half-life of this system.

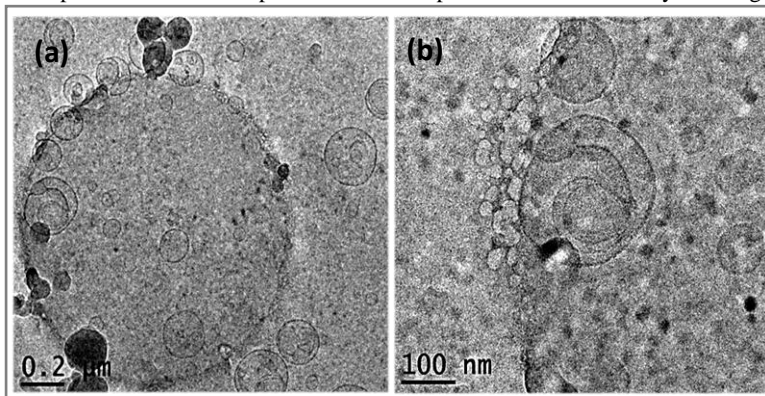


Figure 2: TEM micrographs of the P₁CF₁ formulation at different resolutions showing efficient encapsulation of the peptide in the liposome. Scale bars = 0.2 μm; 100 nm.

| Formulation | Size (nm) | PDI | ZP (mV) | %EE |
|-----------------|------------------|------------------|------------------|------------------|
| Blank liposomes | 164.1 ± 0.11 | 0.290 ± 0.12 | -7.73 ± 0.47 | |
| ACP liposomes | 193.4 ± 0.10 | 0.342 ± 0.12 | -7.67 ± 0.04 | 91.23 ± 0.01 |

Table 1: Particle size, polydispersity Index (PDI), and zeta potential (ZP) of blank liposomes and ACP encapsulated liposomes. Data displayed as mean \pm SD (n = 3).

3.3 Determination of Encapsulation Efficiency Percentage

The analysis of liposome encapsulation efficiency (EE) is an extremely crucial parameter since liposomes are utilized in pharmaceuticals as drug carriers that facilitate drug absorption, targeting effects, and protection of drugs [59]. According to the literature, the EE% is calculated from the difference between the entrapped drug (the total amount of drug added to the liposome formulation) and the untrapped drug (the amount of drug found in the supernatant of the resulting liposome formulation) divided by the total drug added ($EE\% = \frac{\text{total drug added} - \text{free non-entrapped drug}}{\text{total drug added}}$) [60]. In this study, the encapsulation efficiency of the liposome was determined using RP-HPLC at wavelength 220 nm.

The standard curve of the formulation was made by plotting HPLC peak areas against the concentration. The steps indirect method used for the entrapped and untrapped values were reported by Suleiman and coworkers [61], however, the dilutions used in this study were with acetonitrile. The concentrations of the entrapped and untrapped drugs were calculated using the calibration curve with the equation $y=5045.2x$. To measure the amount of active drug loaded in a liposome, the drug would have had to be fully encapsulated by the lipid of the liposome formulation. To determine the EE, the mass ratio between the amount of the drug integrated into the liposome and this ratio was employed in the liposome preparation. The overall entrapment yield was calculated to be

91.23 ± 0.01%, which is relatively high; this was expected as many liposomes have been reported to possess high EE because of their high volume to surface area ratio [9]. The relatively high EE% indicates that the ratio of the used lipids to the ACP was an optimal choice for the formulation. The obtained results from the study revealed high EE and this may be due to many factors, one of them being the effect of probe sonication. According to the literature, liposomal formulations that have been probe-sonicated for longer tend to be more homogenized and hence more susceptible to interacting with surrounding molecules, which greatly influences their enhanced encapsulation efficiency [62]. Additionally, the hydrophilic nature of the peptide used herein could have further facilitated the observed high EE%. This is according to previous studies which have shown that the encapsulation of hydrophilic peptides (as with the one used in this study) in liposomes is expected to be the most efficient due to the electrostatic interaction between the peptide and the liposome surface [61, 63].

3.4 *In vitro* Hemolysis Testing

The *in vivo* application of drugs/drug-loaded nanoformulations entails their transportation via the bloodstream which could lead to adverse effects, such as immunological responses, complex formation with macromolecules, and cell damage [64]. Exposure to chemicals, such as drugs or drug-loaded nanoformulations, can result in an early breakdown of erythrocytes of red blood cells releasing the hemoglobin (Hb), which

can disrupt normal oxygen transport and induce hemolytic anemia/hemolysis [65, 66]. The drugs/drug-loaded nanoformulations may either adsorb on the membrane of the erythrocyte, causing the membrane to distort and become damaged [67]; or they have the ability to cause osmotic lysis by causing holes in the erythrocyte membrane [68]. Thus, it is important to determine if drug-loaded nanoformulations with therapeutic effects induce hemolysis in erythrocytes *in vitro* [69]. To establish this, erythrocytes of sheep red blood cells were exposed to different doses of the ACP encapsulated liposome formulation (P₁CF₁) and evaluated for possible hemolysis [70].

The percentage (%) of erythrocyte hemolysis induced by the P₁CF₁ formulation is shown in Fig 3. Both the graph and the image insert depicted that the formulation was non-toxic to erythrocytes at doses 0.05 and 0.1 mg/ml, suggesting its biocompatibility at these low therapeutic doses. Hemolysis was neglectable at a dose of 0.2 mg/ml and increased with increasing concentration of the P₁CF₁ formulation from doses greater than 0.2 mg/ml up to 0.5 mg/ml. This can be credited to the agglomeration feature of ACP liposomes at higher doses. Moreover, compared to untreated cells (C2), an 88% increase in hemolysis was observed at a dose of 0.5 mg/ml post-treatment, indicating that the formulation had an adverse effect on erythrocytes at higher doses. Overall, these findings indicated that the formulation was non-toxic at low therapeutic concentrations equal to or less than 0.2 mg/ml.

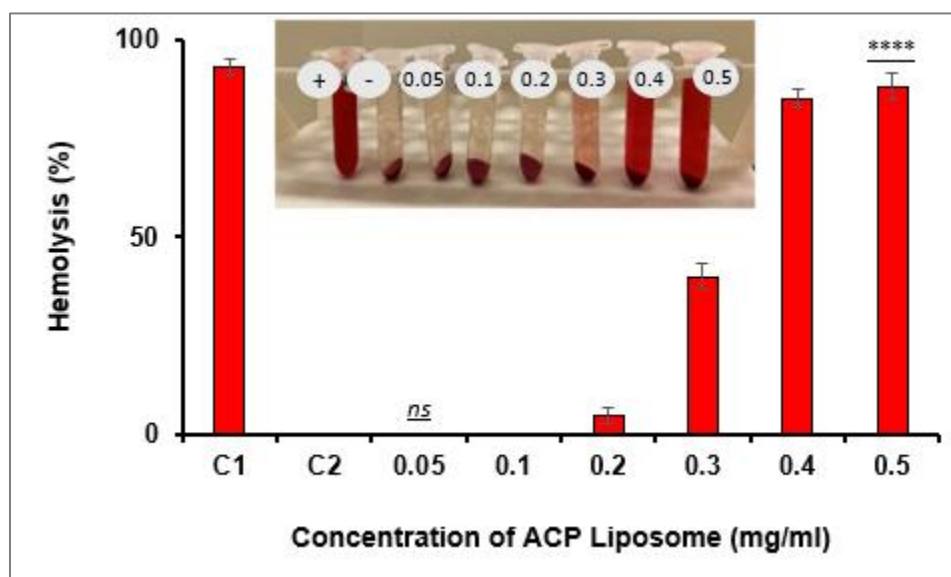


Figure 3: Hemolysis toxicity of the P₁CF₁ formulation towards red blood cells at varying concentrations (0.05 to 0.5 mg/ml). Data is shown as means ± SD (n = 3). The image insert shows the representation of the haemolytic behaviour of RBCs after treatment with P₁CF₁ formulation. C1 denotes control 1 = positive control (+) = RBCs + distilled water; C2 denotes control 2 = negative control (-) = RBCs + PBS. ****p < 0.0001 vs. C2; ns indicates non-statistical significance from C2.

3.5 *In vitro* Drug Release Analysis

To predict the quantity of a drug's accumulation into the bloodstream and tumour sites over time, *in vitro* drug release studies are usually conducted. The *in vitro* drug release profile of the ACP encapsulated liposomes (P₁CF₁ formulation) was assessed using a dialysis bag technique with PBS solutions at pH 6.0 and 7.4 prepared at 37°C for 72 hrs. These pH buffer solutions mimic the basic physiological state and the acidic endosomal cancer cell microenvironment (pH 4-6) [71]. Bare peptide was used as a reference or negative control. There was only 5.1% and 3.7% of

bare peptide released at pH of 7.4 and pH 6.0 respectively at 72 hrs (Figure 8 in the Supplementary Information). This was expected since the peptide was not encapsulated in any nanoparticle, so, its large size could have restricted its release or diffusion across the semipermeable dialysis bag membrane.

Figure 4 displays the release profile of P₁CF₁ formulations and the accumulative release of loaded ACP, which was sustained/controlled, acid-dependent, and exhibited a biphasic release pattern across the time studied. During the first 10 hours, there was a quick release of the APC,

followed by a slow controlled release of the APC for the remaining duration of 72 hrs. A higher ACP release rate of 88% was seen at an acidic pH of 6.0 whereas a slower drug release rate of 79% was seen at a healthy pH of 7.4. The initial burst ACP release may have been caused by the release of the untrapped ACP on the liposome periphery, while the subsequent slow and controlled release may have been caused by the release of the ACP encapsulated inside the liposome [71, 72]. The protonation of the amine groups of the encapsulated ACP (see Fig 1) at acidic pHs results in a conformational change of the liposome, causing swelling, bursting, and releasing of the encapsulated ACP into the buffer solution [73]. Sustained drug release is of high importance for cancer therapeutics as it enables the drugs to be released for longer durations, ensuring a continuous stable dosage of the drug to the tumour sites [74]. The cholesterol present within the liposome also helps to regulate the properties of the lipid bilayer of the liposomes as well as the release of

water-soluble compounds (i.e. the ACP peptide) from liposomes by influencing the fluidity and permeability of the lipid bilayer [1, 75]. The pH-dependent drug release property raises the possibility that this P₁CF₁ formulation could be employed to deliver anticancer drugs specifically to tumours (with an acidic microenvironment) [74, 76]. Additionally, the results indicate that most of the ACP encapsulated within the liposome will remain intact in the plasma (pH 7.4) after injection, greatly decreasing the possibility of any systemic adverse effects on the healthy tissues. Furthermore, the results showed that once inside the tumour cells, the cytosolic release of the ACP-encapsulated liposomes/ P₁CF₁ from the endosome is expected to be quicker due to the lower pH than physiological pH conditions. Consequently, it is hoped that the encapsulation of ACP into liposomes will improve the effectiveness of targeted cancer treatment.

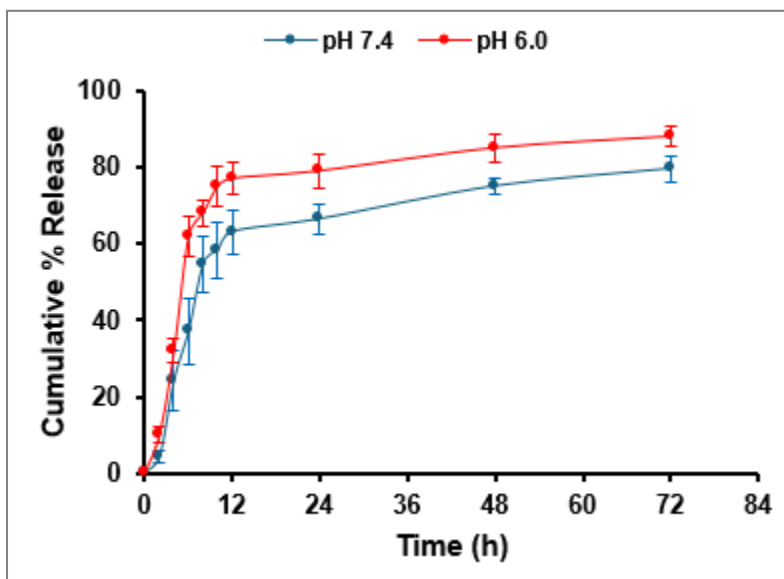


Figure 4: *In vitro* drug release profile of ACP encapsulated liposome in pH 6.0 and 7.4 over 72 hours. Data is shown as mean \pm SD (n = 3).

3.6 *In vitro* Cytotoxicity Analysis

The initial step in assessing a drug delivery system's biocompatibility usually includes the use of cell-culture-based research such as *in vitro* cell viability studies, which typically starts with the assessment of its cytotoxicity profile. The MTT test that was used in this study quantifies metabolically active cells by measuring yellow formazan products produced from the conversion of purple MTT salt by mitochondrial reductase enzyme found in live cells [34]. Untreated cells served as negative controls, azacitidine, a known anticancer drug [77], was used as a positive control.

MCF-7 cancer cells and HEK293 non-cancer cells were treated with ACP-encapsulated liposomes (P₁CF₁), bare peptide, and azacitidine at varying doses ranging from 10 to 200 μ g/ml (Figure 5-6). Following treatment, a drastic decrease in % cell viability ranging between 1.5% and 40% with all tested formulations in MCF-7 cancer cells across the tested doses was observed. At a low dose of 10 μ g/ml, the P₁CF₁ and bare peptide formulations exhibited significantly higher % cell inhibitions of 98.2% and 97.9% respectively, compared to counterpart azacitidine (% cell inhibition of 80%) ($p < 0.0001$) (Figure 5). At a maximum dose of 200 μ g/ml, there was no significant difference between the % cell inhibition of all tested formulations; all formulations were equally potent

to the cells with % cell inhibition ranging between 98.2% and 98.9% ($p < 0.0001$). The calculated IC₅₀ values of the tested formulations were 2.967 μ g/ml for P₁CF₁, 2.955 μ g/ml for bare peptide, and 11.96 μ g/ml for azacitidine (Table 2 and Fig 9a-c in the Supplementary Information). These findings showed that both the P₁CF₁ and bare peptide formulations, were potent to MCF-7 cancer cells as indicated by their low IC₅₀ values, which meant that only a small dose is required to elicit tumour inhibition, compared to the counterpart azacitidine. On the other hand, higher % cell viabilities of greater than 80% were observed in HEK293 cell lines post-treatment with P₁CF₁ at doses equal to or lower than 100 μ g/ml (Figure 6). This suggested that the P₁CF₁ formulation was non-toxic to normal cells at low doses, and was toxic at doses greater than 100 μ g/ml. The estimated IC₅₀ of the P₁CF₁ formulation in HEK239 cells was 135.3 μ g/ml (Table 2 and Fig 9d in the Supplementary Information) meaning a greater amount of the peptide is required to cause toxicity towards this cell line.

Overall, both the P₁CF₁ and the bare peptide inhibited the cell viability of MCF-7 cell lines more than azacitidine. Both the P₁CF₁ and bare peptide there exhibited greater than 90% cytotoxicity towards the cancer cells, with minimum effect on non-cancer cells at low concentrations. The findings suggested that the tested both P₁CF₁ and the bare peptide formulations effectively inhibited the cell in a dose-dependent manner. It

is worth mentioning that though both P₁CF₁ and the bare peptide formulations behaved relatively the same in these *in vitro* cytotoxicity studies in terms of tumour cell inhibition, this might not hold true for *in vivo* studies because much of the bare/naked peptide may be degraded by intracellular and extracellular proteins after administration, while the

opposite might be true with the P₁CF₁ due to the protection the liposomal coat is expected to provide to the encapsulated peptide, which might lead to better performance/higher therapeutic index/cell inhibition. The results correspond with those obtained in hemolysis analyses.

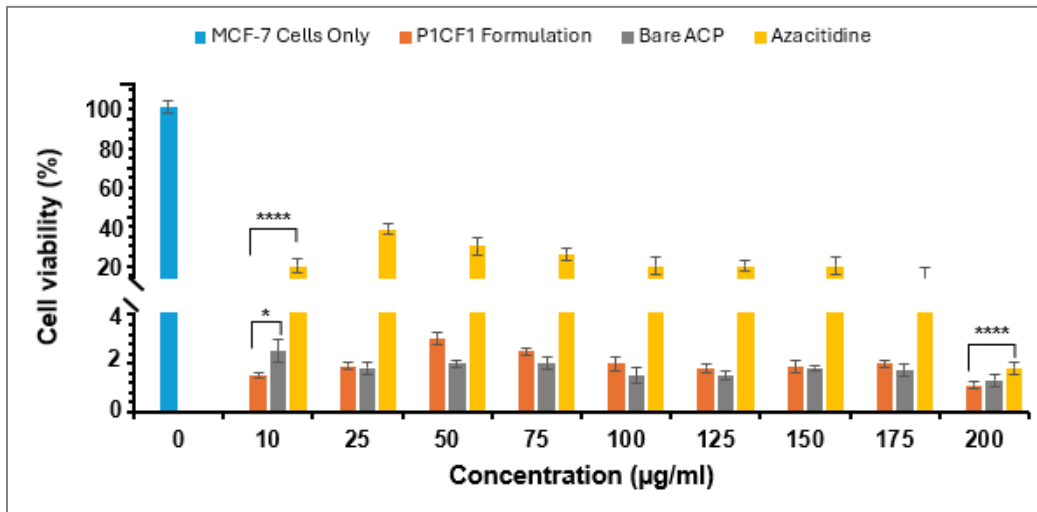


Figure 5: Cytotoxicity of P₁CF₁ formulation, bare ACP, and azacitidine in cancer MCF-7 cell line after 24 hours treatment with different concentrations of 10 – 200 µg/ml. Data is presented as means ± S.D (n = 3). Control (0): untreated cells. P₁CF₁ vs Bare ACP **p* < 0.05, P₁CF₁ and Bare ACP vs azacitidine *****p* < 0.0001, and all formulations vs. control *****p* < 0.0001.

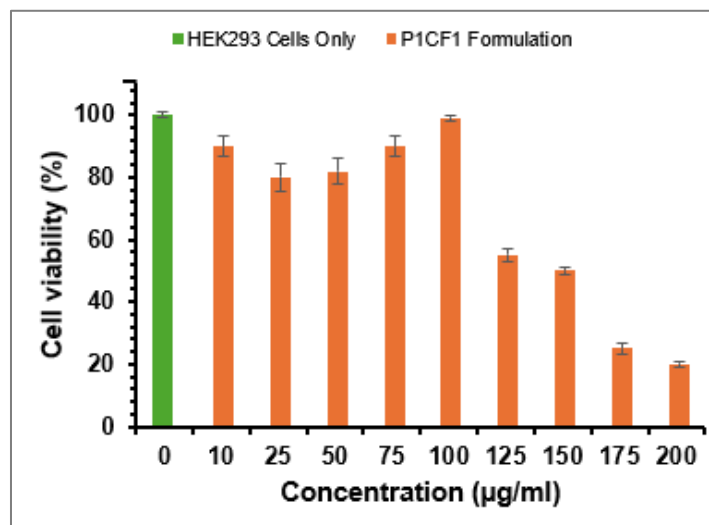


Figure 6: Cytotoxicity of the P₁CF₁ formulation in non-cancer HEK293 cells after 24 hours of treatment with different concentrations of 10 – 200 µg/ml. Data is presented as means ± S.D (n = 3). Control (0): untreated cells.

| Formulation | IC ₅₀ (µg/ml) | |
|--------------------------------|--------------------------|--------------|
| | MCF-7 Cells | HEK293 Cells |
| P ₁ CF ₁ | 2.967 | 135.3 |
| ACP Bare | 2.955 | - |
| Azacitidine | 11.96 | - |

(-) Denotes that IC₅₀ was not determined

3.7 Cell Apoptosis Assay Analysis

Apoptosis induction is critical in cancer therapy research. This is a programmed cell death that helps maintain the balance between cell

growth and cell death. If apoptosis is blocked/prevented for whatever reason, it can result in uncontrolled cell division and the formation of tumours [78]. Apoptosis occurs when cells undergo morphological and

biochemical changes throughout their life cycle. Loss of plasma membrane asymmetry is an early step in the apoptotic process [79].

Herein, flow cytometry and annexin V-FITC/PI assay were employed to detect the apoptosis effect of P₁CF₁, bare ACP, and azacitidine formulations on MCF-7 cancer cells. Flow cytometry allows the investigation of all phases of apoptosis from induction through surface receptors, to the last phases of DNA fragmentation (necrosis) in a single population of cells [80]. The test relies on the capacity of annexin V, a 35–36 kDa phospholipid-binding protein that is dependent on calcium (Ca²⁺) and has a higher affinity for phosphatidylserine (PS) which is found on the inner leaf of the plasma membrane, to attach to the membrane phospholipid PS that is exposed at the cell surface in the early to mid-phases of apoptosis [80]. When used in conjunction with a viability dye, such as the DNA-binding dye PI, apoptotic and necrotic cells may be differentiated [80, 81]. Necrosis is determined by measuring the plasma membrane's permeability to PI, a typically impenetrable fluorescent dye. Apoptosis is determined by detecting the externalization of anionic PS on the plasma membrane with FITC-tagged annexin V [80]. FITC is a green, fluorescent molecule with a 491 nm excitation peak and a 516 nm emission peak [82].

The simultaneous staining of cells with annexin V-FITC and PI allowed for the classification of cells into four quadrats (Q): necrotic cells (Q1), late apoptotic cells (Q2), viable cells (Q3), and early apoptotic cells (Q4) (Fig 7a-b and Table 3 in the Supplementary Information). Fig 7(a-b) shows that the apoptosis effect of MCF-7 cells was significantly increased following treatment with all tested formulations (P₁CF₁, bare ACP, and azacitidine) compared with the controls (MCF-7 only) ($****p < 0.0001$). Both P₁CF₁ and bare ACP induced more apoptosis with the P₁CF₁ displaying the highest effect ($6.95 \pm 0.23\%$ and $5.42 \pm 0.45\%$ respectively) compared with azacitidine ($4.55 \pm 0.21\%$). The apoptosis effect induced by both P₁CF₁ and bare ACP could be attributed to their interaction with the mitochondrial membrane, which subsequently causes membrane rupture leading to the release of pro-apoptosis factors (such as cytochrome C, apoptotic peptidase activating factor 1, caspase-9, and 3) into the cytoplasm which then binds with the cell membrane and disrupts it by forming pores leading to cell death/cell membrane disruption mediated apoptosis [83-85]. The findings corroborate with those obtained by MTT assay.

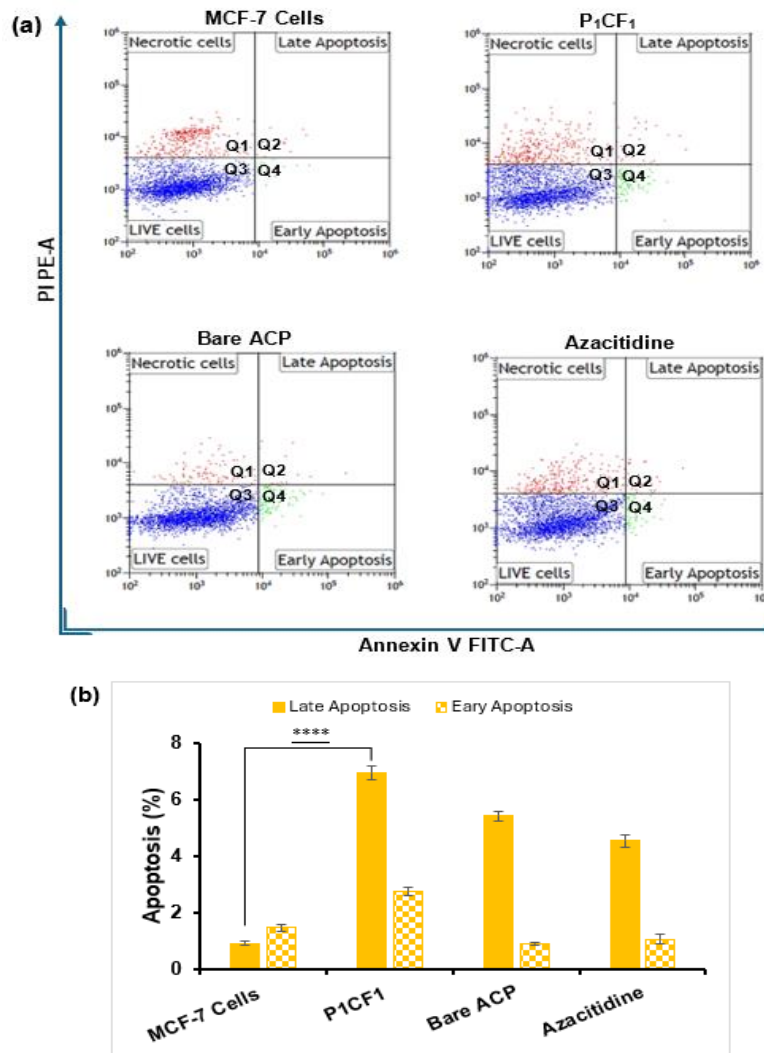


Figure 7: Flow cytometry apoptosis analysis of MCF-7 cells after treatment with P₁CF₁, bare ACP, and azacitidine and staining with Annexin V-FITC and PI. (a) Annexin V-FITC/PI PE-A contour diagrams of MCF-7 cells; the graphs depict typical apoptotic outcomes. Early and late apoptosis were

measured and indicated in gates Q2 and Q4, respectively. (b) Comparison of early and late apoptotic cell percentages in Q2 and Q4 gates of tested formulations. Data is presented as mean \pm S.D (n = 3). Control: untreated cells/MCF-7 only. **** $p < 0.0001$ vs. control.

4. Conclusion

A novel anticancer peptide-encapsulated liposome formulation (P₁CF₁) was successfully designed and formulated using *in silico* and thin-film layer rehydration methods, respectively. The formulation had optimal physicochemical characteristics for efficient drug delivery *in vitro*, as well as improved encapsulation efficiency. Encapsulating the novel anticancer peptide in a liposome delivery system improved its *in vitro* bioavailability and biocompatibility. At acidic pH conditions, the formulation also demonstrated increased controlled and sustained *in vitro* anticancer peptide release, implying that treatment at the target tumour sites might be prolonged. The P₁CF₁ formulation had higher cytotoxicity than the known anticancer drug, azacitidine in cancer cells, with a percentage cell inhibition of 98.2%. However, it was ineffective in non-cancer cells (% cell inhibition < 20%), especially at low therapeutic dosages. Furthermore, the P₁CF₁ formulation induced a higher apoptosis rate in the MCF-7 cell line, compared to counterparts, bare peptide and free azacitidine. These positive characteristics indicate potential *in vivo* applicability. Thus, future research can include *in vivo* evaluation of this unique formulation.

Author contributions: project conceptualization and designing, Lusanda Mtetwa, Nkeiruka Igbokwe, and Mbuso Faya.; resources, Mbuso Faya and Anil Chuturgoon.; data collection.; Lusanda Mtetwa.; data curation and software, Lusanda Mtetwa, Nkeiruka Igbokwe, Aviwe Ntsethe, Makabongwe Mazibuko and Terisha Ghazi.; writing - initial draft preparation, Lusanda Mtetwa.; writing - final draft preparation, Lusanda Mtetwa, Nkeiruka Igbokwe and Londiwe Simphiwe Mbatha.; final draft reviewing and editing, Londiwe Simphiwe Mbatha and Mbuso Faya.; funding acquisition, Mbuso Faya and Anil Chuturgoon.; project supervision and administration, Mbuso Faya. All authors have read and agreed to the published version of the manuscript.

Acknowledgments and funding: The University of KwaZulu Natal, College of Health Science is acknowledged for financial support as well as the National Research Foundation (grant number: 138291). Any opinions, findings, conclusions, or recommendations expressed in this article are those of the authors.

Data availability: Supporting data are available from the corresponding author upon request.

Conflicts of interest: The authors declare no conflict of interest.

Declarations: Ethical approval, is not applicable.

Supplementary information: Fig 8. *In vitro* drug release profile of bare ACP in pH 7.4 and pH 6.0 over 72 hours. Data is shown as mean \pm SD (n = 3); Fig 9(a-d). IC₅₀ estimated values of P₁CF₁ (a), bare ACP (b), and azacitidine (c) in MCF-7 cell lines; IC₅₀ estimated value of P₁CF₁ (d) in HEK293; Table 3. Flow cytometry analysis; gate total percentages of MCF-7 only, P₁CF₁, Bare ACP, and Azacitidine.

References

1. Sonju JJ, Dahal A, Singh SS, Jois SD (2021) Peptide-functionalized liposomes as therapeutic and diagnostic tools for cancer treatment. *J Control Release* 329: 624-644. <https://doi.org/10.1016/j.jconrel.2020.09.055>
2. Akanda M, Mithu MSH, Douroumis D (2023) Solid lipid nanoparticles: an effective lipid-based technology for cancer treatment. *J Drug Deliv Sci Technol* 104709.
3. Li YJ, Lei YH, Yao N, Wang CR, Hu N, Ye WC, Zhan DM, Chen ZS (2017) Autophagy and multidrug resistance in cancer. *Chin J Cancer* 36: 1-10. <https://doi.org/10.1186/s40880-017-0219-2>
4. Singh SK, Singh S, Lillard Jr JW, Singh R (2017) Drug delivery approaches for breast cancer. *Int J Nanomed* 12: 6205-6218. <https://doi.org/10.2147/IJN.S140325>
5. Mokhatri-Hesari P, Montazeri A (2020) Health-related quality of life in breast cancer patients: review of reviews from 2008 to 2018. *HRQLO* 18: 1-25. <http://dx.doi.org/10.1186/s12955-020-01591-x>
6. Teixeira S, Carvalho MA, Castanheira EM (2022) Functionalized liposome and albumin-based systems as carriers for poorly water-soluble anticancer drugs: an updated review. *Biomedicines* 10(2): 486. <https://doi.org/10.3390/biomedicines10020486>
7. Liu R, Zhou J, Yang S, Zhang Z (2018) Efficacy and safety of pegylated liposomal doxorubicin-based chemotherapy of AIDS-related Kaposi's Sarcoma: a meta-analysis. *Am J Ther* 25(6): e719-e721. <https://doi.org/10.1097/MJT.0000000000000736>
8. Torchilin VP (2005) Recent advances with liposomes as pharmaceutical carriers. *Nat Rev Drug Discov* 4(2): 145-160. <https://doi.org/10.1038/nrd1632>.
9. Dua, JS, Rana AC, and Bhandari A (2012) Preparation, optimization, characterization of liposomes containing serration-peptidase for oral delivery. *Int J Pharm Stud Res. E-ISSN* 2229-4619
10. García-Pinel B, Porras-Alcalá C, Ortega-Rodríguez A, Sarabia F, Prados J, Melguizo C, López-Romero JM (2019) Lipid-based nanoparticles: application and recent advances in cancer treatment. *Nanomaterials* 9(4): 638. <https://doi.org/10.3390/nano9040638>.
11. Shah S, Dhawan V, Holm R, Nagarsenker MS, Perrie Y (2020) Liposomes: advancements and innovation in the manufacturing process. *Advanced Drug Deliv Rev* 154: 102-122. <https://doi.org/10.1016/j.addr.2020.07.002>.
12. Andra VVSNL, Pammi SVN, Bhatraju LVKP, Ruddaraju, LK (2022) A comprehensive review on novel liposomal methodologies, commercial formulations, clinical trials and patents. *Bionanoscience* 12(1): 274-291. <https://doi.org/10.1007/s12668-022-00941-x>.
13. Sharma G, Anabousi S, Ehrhardt C, Ravi Kumar MNV (2006) Liposomes as targeted drug delivery systems in the treatment of breast cancer. *J Drug Target* 14(5): 301-310.

14. Bulbake U, Kommineni N, Khan W (2020) Liposomal drug delivery system and its clinically available products. In Handbook of Materials for Nanomedicine, 1st Edn. Jenny Stanford Publishing, New York, pp 121-172. <https://doi.org/10.1201/9781003045076-4>
15. Lee TY, Lin CT, Kuo SY, Chang DK, Wu HC (2007) Peptide-mediated targeting to tumor blood vessels of lung cancer for drug delivery. *Cancer Res* 67(22): 10958-10965. <https://doi.org/10.1158/0008-5472.CAN-07-2233>.
16. Lo A, Lin CT, Wu HC (2008) Hepatocellular carcinoma cell-specific peptide ligand for targeted drug delivery. *Mol Cancer Ther* 7(3): 579-589. <https://doi.org/10.1158/1535-7163.MCT-07-2359>.
17. Liang Z, Du L, Zhang E, Zhao Y, Wang W, Ma P, Dai M, Zhao Q, Xu H, Zhang S, Zhen Y (2021) Targeted-delivery of siRNA via a polypeptide-modified liposome for the treatment of gp96 over-expressed breast cancer. *Mater Sci Eng C*. 121: 111847. <https://doi.org/10.1016/j.msec.2020.111847>
18. Zahmatkeshan M, Gheybi F, Rezayat SM, Jaafari MR (2016) Improved drug delivery and therapeutic efficacy of PEGylated liposomal doxorubicin by targeting anti-HER2 peptide in murine breast tumor model. *Eur J Pharm Sci* 86: 125-135. <https://doi.org/10.1016/j.ejps.2016.03.009>
19. Ding Y, Cui W, Sun D, Wang GL, Hei Y, Meng S, Chen JH, Xie Y, Wang ZQ (2017) In vivo study of doxorubicin-loaded cell-penetrating peptide-modified pH-sensitive liposomes: biocompatibility, bio-distribution, and pharmacodynamics in BALB/c nude mice bearing human breast tumors. *Drug Des Devel Ther* 3105-3117. <https://doi.org/10.2147/DDDT.S149814>
20. Xia T, He Q, Shi K, Wang Y, Yu Q, Zhang L, Zhang Q, Gao H, Ma L, Liu J (2018) Losartan loaded liposomes improve the antitumor efficacy of liposomal paclitaxel modified with pH sensitive peptides by inhibition of collagen in breast cancer. *Pharm Dev Technol* 23(1): 13-21. <https://doi.org/10.1080/10837450.2016.1265553>
21. Kim B, Shin J, Wu J, Omstead DT, Kiziltepe T, Littlepage LE, Bilgicer B (2020) Engineering peptide-targeted liposomal nanoparticles optimized for improved selectivity for HER2-positive breast cancer cells to achieve enhanced in vivo efficacy. *J Control Release* 322: 530-541. <https://doi.org/10.1016/j.jconrel.2020.04.010>
22. Bhunia D, Saha A, Adak A, Das G, Ghosh S (2016) A dual functional liposome specifically targets melanoma cells through integrin and ephrin receptors. *RSC Adv* 6(114): 113487-113491. <https://doi.org/10.1039/C6RA23864E>
23. Yoon HY, Kwak SS, Jang MH, Kang MH, Sung SW, Kim CH, Kim SR, Yeom DW, Kang MJ, Choi YW (2017) Docetaxel-loaded RIPL peptide (IPLVVPLRRRRRRRRC)-conjugated liposomes: drug release, cytotoxicity, and antitumor efficacy. *Int J Pharm* 523(1): 229-237. <https://doi.org/10.1016/j.ijpharm.2017.03.045>
24. Zhang L, Ren Y, Wang Y, He Y, Feng W, Song C (2018) Pharmacokinetics, distribution and anti-tumor efficacy of liposomal mitoxantrone modified with a luteinizing hormone-releasing hormone receptor-specific peptide. *Int J Nanomedicine* 13: 1097-1105. <https://doi.org/10.2147/IJN.S150512>
25. Gaspar D, Veiga AS, Castanho MA (2013) From antimicrobial to anticancer peptides: a review. *Front Microbiol* 4: 294. <https://doi.org/10.3389/fmicb.2013.00294>
26. González-Montoya M, Cano-Sampedro E, Mora-Escobedo R (2017) Bioactive peptides from legumes as anticancer therapeutic agents. *Int J Cancer Clin Res* 4(081): 56. <https://doi.org/10.23937/2378-3419/1410081>
27. Tyagi A, Tuknait A, Anand P, Gupta S, Sharma M, Mathur D, Joshi A, Singh S, Gautam A, Raghava GP (2015) CancerPPD: a database of anticancer peptides and proteins. *Nucleic Acids Res* 43(D1): D837-D843. <https://doi.org/10.1093/nar/gku892>
28. [Lombardo D, Kiselev MA (2022) Methods of liposomes preparation: formation and control factors of versatile nanocarriers for biomedical and nanomedicine application. *Pharmaceutics* 14(3): 543. <https://doi.org/10.3390/pharmaceutics14030543>
29. Rojas-Mancilla E, Oyarce A, Verdugo V, Zheng, Z, Ramírez-Tagle R (2015) The cluster [Re6Se8I6] 3- induces low hemolysis of human erythrocytes in vitro: protective effect of albumin. *Int J Mol Sci* 16(1): 1728-1735. <https://doi.org/10.3390/ijms16011728>
30. Ayllon M, Abatchev G, Bogard A, Whiting R, Hobdey SE, Fologea D (2021) Liposomes prevent in vitro hemolysis induced by streptolysin O and lysenin. *Membranes* 11(5): 364. <https://doi.org/10.3390/membranes11050364>
31. Seil JT, Webster TJ (2012) Antimicrobial applications of nanotechnology: methods and literature. *Int J Nanomedicine* 2767-2781. <https://doi.org/10.2147/IJN.S24805>
32. Das S, Ng WK, Tan RB (2012) Are nanostructured lipid carriers (NLCs) better than solid lipid nanoparticles (SLNs): development, characterizations and comparative evaluations of clotrimazole-loaded SLNs and NLCs?. *Eur J Pharm Sci* 47(1), 139-151. <https://doi.org/10.1016/j.ejps.2012.05.010>
33. Mohan J, Sheik Abdul N, Nagiah S, Ghazi T, Chuturgoon AA (2022) Fumonisin B2 induces mitochondrial stress and mitophagy in human embryonic kidney (Hek293) cells—a preliminary study. *Toxins* 14(3): 171. <https://doi.org/10.3390/toxins14030171>
34. Mbatha L, Chakravorty S, B de Koning C, AL van Otterlo W, Arbuthnot P, Ariatti M, Singh M (2016) Spacer length: A determining factor in the design of galactosyl ligands for hepatoma cell-specific liposomal gene delivery. *Curr Drug Deliv* 13(6): 935-945.
35. Inoue S, Arai N, Tomihara K, Takashina M, Hattori Y, Noguchi M (2015) Extracellular Ca²⁺-dependent enhancement of cytotoxic potency of zoledronic acid in human oral cancer cells. *Eur J Pharmacol* 761: 44-54. <https://doi.org/10.1016/j.ejphar.2015.04.032>
36. De Cena GL, Scavassa BV, Conceição K (2022) In silico prediction of anti-infective and cell-penetrating peptides from *Thalassophryne nattereri* natterin toxins. *Pharmaceutics* 15(9): 1141.
37. Thundimadathil J (2012) Cancer treatment using peptides: current therapies and future prospects. *J Amino Acids* 2012(1): 967347. <https://doi.org/10.1155/2012/967347>
38. Langel Ü (2015) Cell-penetrating peptides. *Methods Mol Biol* 1324: v-viii. <https://doi.org/10.1007/978-1-4939-2806-4>

39. Gabernet G, Müller AT, Hiss JA, Schneider G (2016) Membranolytic anticancer peptides. *MedChemComm* 7(12): 2232-2245.
40. Owen DR (2005) Short bioactive peptides. U.S. Patent 6,875,744. Washington, DC: U.S. Patent and Trademark Office. Link: <https://patents.google.com/patent/US6875744B2/en>. Accessed 10 November 2023.
41. Gautam, A., Chaudhary, K., Kumar, R., Sharma, A., Kapoor, P., Tyagi, A., and Raghava, G.P., 2013. In silico approaches for designing highly effective cell penetrating peptides. *J Transl Med* 11: 1-12.
42. Huang KY, Tseng YJ, Kao HJ, Chen CH, Yang HH, Weng SL (2021) Identification of subtypes of anticancer peptides based on sequential features and physicochemical properties. *Sci Rep* 11(1): 13594. <https://doi.org/10.1038/s41598-021-93124-9>
43. Dennison SR, Whittaker M, Harris F, Phoenix DA (2006) Anticancer α -helical peptides and structure/function relationships underpinning their interactions with tumour cell membranes. *Curr Protein Pept Sci* 7(6): 487-499. <https://doi.org/10.2174/138920306779025611>
44. Hoshyar N, Gray S, Han H, Bao G (2016) The effect of nanoparticle size on in vivo pharmacokinetics and cellular interaction. *Nanomedicine* 11(6): 673-692. <https://doi.org/10.2217/nnm.16.5>
45. Schwendener RA (2007) Liposomes in biology and medicine. *Adv Exp Med Biol* 117-128. <https://doi.org/10.1007/978-1-4939-6591-5>
46. Azzam T, Domb AJ (2004) Current developments in gene transfection agents. *Curr Drug Deliv* 1(2): 165-193. <https://doi.org/10.2174/1567201043479902>
47. Rejman J, Oberle V, Zuhorn IS, Hoekstra D (2004) Size-dependent internalization of particles via the pathways of clathrin- and caveolae-mediated endocytosis. *Biochem J* 377(1): 159-169. <https://doi.org/10.1042/bj20031253>
48. Grosse S, Aron Y, Thévenot G, François D, Monsigny M, Fajac I (2005) Potocytosis and cellular exit of complexes as cellular pathways for gene delivery by polycations. *J Gene Med* 7(10): 1275-1286. <https://doi.org/10.1002/jgm.772>
49. Panwar P, Pandey B, Lakhera PC, Singh KP (2010) Preparation, characterization, and in vitro release study of albendazole-encapsulated nanosize liposomes. *Int J Nanomed* 101-108. <https://doi.org/10.2147/ijn.s8030>
50. Hong SS, Lim SJ (2015) Laboratory scale production of injectable liposomes by using cell disruptor to avoid the probe sonication process. *J Pharm Investig* 45: 73-78. <https://doi.org/10.1007/s40005-014-0146-z>
51. Ockun MA, Baranauskaitė J, Uner B, Kan Y, Kırmızıbekmez H (2022) Preparation, characterization and evaluation of liposomal-freeze dried anthocyanin-enriched *Vaccinium arctostaphylos* L. fruit extract incorporated into fast dissolving oral films. *J Drug Deliv Sc Technol* 72: 103428. <https://doi.org/10.1016/j.jddst.2022.103428>
52. Sebaaly C, Charcosset C, Stainmesse S, Fessi H, Greige-Gerges H (2016) Clove essential oil-in-cyclodextrin-in-liposomes in the aqueous and lyophilized states: From laboratory to large scale using a membrane contactor. *Carbohydr Polym* 138, 75-85. <https://doi.org/10.1016/j.carbpol.2015.11.053>
53. Mignet N, Seguin J, Romano MR, Brullé L, Touil YS, Scherman D, Bessodes M, Chabot GG (2012) Development of a liposomal formulation of the natural flavonoid fisetin. *Int J Pharm* 423(1): 69-76. <https://doi.org/10.1016/j.ijpharm.2011.04.066>
54. Gharib R, Auezova L, Charcosset C, Greige-Gerges H (2017) Drug-in-cyclodextrin-in-liposomes as a carrier system for volatile essential oil components: application to anethole. *Food Chem* 218: 365-371. <https://doi.org/10.1016/j.foodchem.2016.09.110>
55. Honary S, Zahir F (2013) Effect of zeta potential on the properties of nano-drug delivery systems-a review (Part 1). *Trop J Pharm Res* 12(2): 255-264. <https://doi.org/10.4314/tjpr.v12i2.20>
56. Malinga T, Kudanga T, Mbatha LS (2021) Stealth doxorubicin conjugated bimetallic selenium/silver nanoparticles for targeted cervical cancer therapy. *ANSN* 12: 045006. <https://doi.org/10.1088/2043-6262/ac389c>
57. Ascenso A, Cruz M, Euletério C, Carvalho FA, Santos NC, Marques HC, Simoes S (2013) Novel tretinoin formulations: a drug-in-cyclodextrin-in-liposome approach. *J Liposome Res* 23(3): 211-219. <https://doi.org/10.3109/08982104.2013.788026>
58. Rafiee Z, Barzegar M, Sahari MA, Maherani B (2017) Nanoliposomal carriers for improvement the bioavailability of high-valued phenolic compounds of pistachio green hull extract. *Food Chem* 220: 115-122. <https://doi.org/10.1016/j.foodchem.2016.09.207>
59. Ran C, Chen D, Xu M, Du C, Li Q, Jiang Y (2016) A study on characteristic of different sample pretreatment methods to evaluate the entrapment efficiency of liposomes. *J Chromatogr B* 1028: 56-62. <https://doi.org/10.1016/j.jchromb.2016.06.008>
60. Pitaksuteepong T, Davies NM, Tucker IG, Rades T (2002) Factors influencing the entrapment of hydrophilic compounds in nanocapsules prepared by interfacial polymerisation of water-in-oil microemulsions. *Eur J Pharm Biopharm* 53(3): 335-342. [https://doi.org/10.1016/S0939-6411\(01\)00245-4](https://doi.org/10.1016/S0939-6411(01)00245-4)
61. Suleiman E, Damm D, Batzoni M, Temchura V, Wagner A, Überla K, Vorauer-Uhl K (2019) Electrostatically driven encapsulation of hydrophilic, non-conformational peptide epitopes into liposomes. *Pharmaceutics* 11(11): 619. <https://doi.org/10.3390/pharmaceutics11110619>
62. He Y, Luo L, Liang S, Long M, Xu H (2019) Influence of probe-sonication process on drug entrapment efficiency of liposomes loaded with a hydrophobic drug. *Int J Polym Mater Polym Biomater* 68(4): 193-197. <https://doi.org/10.1080/00914037.2018.1434651>
63. Shariat S, Badiie A, Jaafari MR, Mortazavi SA (2014) Optimization of a method to prepare liposomes containing HER2/Neu-derived peptide as a vaccine delivery system for breast cancer. *Iran J Pharm Res* 13: 15.
64. Jin X, Chalmers JJ, Zborowski M (2012) Iron transport in cancer cell culture suspensions measured by cell magnetophoresis. *Analy Chem* 84(10): 4520-4526. <https://doi.org/10.1021/ac3004677>
65. Hebbel RP, Leung A, Mohandas N (1990) Oxidation-induced changes in microrheologic properties of the red blood cell

- membrane. *Blood* 76 (5): 1015–1020. <https://doi.org/10.1182/blood.V76.5.1015.1015>
66. Duchnowicz, P., Koter, M. and Duda, W., 2002. Damage of erythrocyte by phenoxyacetic herbicides and their metabolites. *Pestic Biochem Phys* 74(1): 1-7. [https://doi.org/10.1016/S0048-3575\(02\)00139-6](https://doi.org/10.1016/S0048-3575(02)00139-6)
67. Tran CL, Buchanan D, Cullen RT, Searl A, Jones AD, Donaldson K (2000) Inhalation of poorly soluble particles. II. Influence of particle surface area on inflammation and clearance. *Inhal Toxicol* 12(12): 1113-1126. <https://doi.org/10.1080/08958370050166796>
68. Kwon T, Woo HJ, Kim YH, Lee HJ, Park KH, Park S, Youn B (2012) Optimizing hemocompatibility of surfactant-coated silver nanoparticles in human erythrocytes. *J Nanosci Nanotechnol* 12(8), 6168-6175. <https://doi.org/10.1166/jnn.2012.6433>
69. Love SA, Thompson JW, Haynes CL (2012) Development of screening assays for nanoparticle toxicity assessment in human blood: preliminary studies with charged Au nanoparticles. *Nanomedicine* 7(9): 1355-1364. <https://doi.org/10.2217/nnm.12.17>
70. Liao KH, Lin YS, Macosko CW, Haynes CL (2011) Cytotoxicity of graphene oxide and graphene in human erythrocytes and skin fibroblasts. *ACS Appl Mater Interfaces* 3(7): 2607-2615. <https://doi.org/10.1021/am200428v>
71. Xia Y, Xu T, Wang C, Li Y, Lin Z, Zhao M, Zhu B (2018) Novel functionalized nanoparticles for tumor-targeting co-delivery of doxorubicin and siRNA to enhance cancer therapy. *Int J Nanomed* 143-159. <https://doi.org/10.2147/IJN.S148960>
72. Rafiei P, Haddadi A (2017) Docetaxel-loaded PLGA and PLGA-PEG nanoparticles for intravenous application: pharmacokinetics and biodistribution profile. *Int J Nanomed* 935-947. <https://doi.org/10.2147/IJN.S121881>
73. Islam A, Yasin T (2012) Controlled delivery of drug from pH sensitive chitosan/poly (vinyl alcohol) blend. *Carbohydr Polym* 88(3): 1055-1060. <https://doi.org/10.1016/j.carbpol.2012.01.070>
74. Amjadi I, Rabiee M, Hosseini MS, Mozafari M (2012) Synthesis and characterization of doxorubicin-loaded poly (lactide-co-glycolide) nanoparticles as a sustained-release anticancer drug delivery system. *Appl Biochem Biotechnol* 168: 1434-1447. <https://doi.org/10.1007/s12010-012-9868-4>
75. Kaddah S, Khreich N, Kaddah F, Charcosset C, Greige-Gerges H (2018) Cholesterol modulates the liposome membrane fluidity and permeability for a hydrophilic molecule. *Food Chem Toxicol* 113: 40-48. <https://doi.org/10.1016/j.fct.2018.01.017>
76. Mishra, S.K. and Kannan, S., 2017. Doxorubicin-conjugated bimetallic silver–gadolinium nanoalloy for multimodal MRI-CT-optical imaging and pH-responsive drug release. *ACS Biomater Sc Eng* 3(12): 3607-3619. <https://doi.org/10.1021/acsbiomaterials.7b00498>
77. Xiong H, Qiu H, Zhuang L, Xiong H, Jiang R, Chen Y (2009) Effects of 5-Aza-CdR on the proliferation of human breast cancer cell line MCF-7 and on the expression of Apaf-1 gene. *J Huazhong Univ Sc Technol* 29: 498-502. <https://doi.org/10.1007/s11596-009-0421-9>
78. Pfeffer CM, Singh AT (2018) Apoptosis: a target for anticancer therapy. *Int J Mol Sc* 19(2): 448. <https://doi.org/10.3390/ijms19020448>
79. Mbatha LS, Akinyelu J, Chukwuma CI, Mokoena MP, Kudanga T (2023) Current trends and prospects for application of green synthesized metal nanoparticles in cancer and COVID-19 therapies. *Viruses* 15(3): 741. <https://doi.org/10.3390/v15030741>
80. Cummings BS, Schnellmann RG (2004) Measurement of cell death in mammalian cells. *Curr Protoc Pharmacol* 25(1): 12-8. <https://doi.org/10.1002/0471141755.ph1208s25>
81. Riccardi C, Nicoletti I (2006) Analysis of apoptosis by propidium iodide staining and flow cytometry. *Nat Protoc* 1(3), 1458-1461. <https://doi.org/10.1038/nprot.2006.238>
82. McCarthy DA (2007) Fluorochromes and fluorescence. *Flow Cytometry: Principles and Applications* 59-112. https://doi.org/10.1007/978-1-59745-451-3_3
83. Garrido C, Galluzzi L, Brunet M, Puig PE, Didelot C, Kroemer G (2006) Mechanisms of cytochrome c release from mitochondria. *Cell Death Differ* 13(9): 1423-1433. <https://doi.org/10.1038/sj.cdd.4401950>
84. Kolbrink B, Riebeling T, Kunzendorf U, Krautwald S (2020) Plasma membrane pores drive inflammatory cell death. *Front Cell Dev Biol* 8: 817. <https://doi.org/10.3389/fcell.2020.00817>
85. Shoshan-Barmatz V, Arif T, Shteinfer-Kuzmine A (2023) Apoptotic proteins with non-apoptotic activity: expression and function in cancer. *Apoptosis* 28(5): 730-753. <https://doi.org/10.1007/s10495-023-01835-3>



This work is licensed under Creative Commons Attribution 4.0 License

To Submit Your Article Click Here:

[Submit Manuscript](#)

DOI:10.31579/2690-4861/589

Ready to submit your research? Choose Auctores and benefit from:

- fast, convenient online submission
- rigorous peer review by experienced research in your field
- rapid publication on acceptance
- authors retain copyrights
- unique DOI for all articles
- immediate, unrestricted online access

At Auctores, research is always in progress.

Learn more <https://auctoresonline.org/journals/international-journal-of-clinical-case-reports-and-reviews>